ELSEVIER

Journal of Nuclear Materials 258–263 (1998) 215–225

journal of nuclear materials

Current status of SiC/SiC composites R&D

P. Fenici [a], A.J. Frias Rebelo [a,*], R.H. Jones [b], A. Kohyama [c], L.L. Snead [d]

[a] *European Commission, JRC, Institute for Advanced Materials, Tp 202, 21020 Ispra (VA), Italy*
[b] *Pacific Northwest National Laboratory, P.O. Box 999 Richland, WA 99532, USA*
[c] *Kyoto University, Institute for Advanced Energy, Kyoto, Japan*
[d] *Oak Ridge National Laboratory, Oak Ridge, TN 37831-6087, USA*

Abstract

Advantages of SiC-based ceramic matrix composites (CMCs) as structural materials in fusion applications rely on their high-temperature properties and stability, low density and reduced neutron activation. In recent years, experimental activities on industrial SiC CMCs have highlighted their main features under irradiation and provided important guidelines for further development of a radiation compliant material. Parallel efforts included design studies, development of advanced fibres and interfaces, alternative composite processing methods and joint development. In this paper, the current status of SiC/SiC R&D is reported and it is demonstrated that future activities require a strong collaboration with the industry as well as common efforts involving the different laboratories.

1. Introduction

Recent years have shown increasing activity for the characterisation of silicon carbide (SiC) based ceramic matrix composites (CMCs) envisaging their application in future fusion power reactors (FPR) [1–3]. Interest in fusion power applications has been based on the low activation of SiC, as well as its dimensional stability under irradiation for temperatures up to 1273 K [1–3]. Availability of small diameter fibres, with moderate high-temperature stability, has allowed the production of CMCs with relatively predictable thermo-mechanical behaviour [3,4], overcoming the brittle behaviour associated to monolithic ceramics.

In the initial section of this paper, current design studies, which anticipate how a CMC structure is applied in a FPR, are summarised. Activation calculations and related experimental activities are outlined, continuing from studies performed on Nicalon™ Ceramic Grade (CG) fibre/SiC composites, with a carbon interface (0.1–0.2 μm), produced by chemical vapour infiltration (CVI). These materials represent the state-of-the-art of industrial CMCs and, whilst alternative production routes (referred in a later section) are available, CVI is the most extensively studied and has provided the main guidelines for R&D of a high-temperature, radiation resistant composite. In the following section, the main results of the irradiation response of Nicalon™ CG fibre/SiC (CVI) are discussed, illustrating its current limitations and introducing recent work on advanced SiC fibres, interfaces or alternative CMCs production routes. Moreover, the necessity of reliable joining procedures is also mentioned, summarising some existing approaches able to meet feasibility requirements for a large SiC_f/SiC composite structure.

2. Design studies

Design projects for FPRs have been carried out considering SiC/SiC composites as a structural material [5–8], attempting both to establish priorities for the development of properties in available materials and to address requirements for component fabrication and assembly. The main parameters for breeding blanket designs relying on SiC_f/SiC composites as a structural material are shown in Table 1.

* Corresponding author. Tel.: +39 332 789768; fax: +39 332 789 434; e-mail: artur.rebelo@jrc.it.

0022-3115/98/$19.00
PII: S0022-3115(98)00303-1

Table 1
Main parameters of SiC/SiC blanket studies

	ARIES-I	DREAM	TAURO
Surf. heat flux (MW/m^2)	0.5	Not reported	0.5
Neutron wall load (MW/m^2)	3.3	5	2
Breeding material	Li_2ZrO_3 (pebbles)	Li_2O (pebbles)	Pb17Li (Liquid)
Neutron multiplier	Be	Be	Pb17Li
Reference composite	SiC/SiC 2-D, 3-D	SiC/SiC 3-D (Guipex)	SiC/SiC 3-D (Hi-Nicalon)
FW protection	SiC CVD	SiC CVD	SiC CVD
Mechanical properties			
Stresses (MPa)			
Primary	140	200	300
Secondary	190		
Young's Modulus (GPa)	E_x:364; E_y:360	200	200
Poisson ratio	0.16	0.2	
Coef. thermal expansion ($\times 10^{-6}$ K^{-1})	α_x:4.4; α_y:4.3	3.3	4
Coolant	He (10 MPa)	He (10 MPa)	Pb17Li(2 MPa)
Inlet/outlet temperatures (K)	623/923	973/1173	528/948
Thermal conductivity (W/mK)	12–15	15	15

For the ARIES-I design, the blanket modules consist of a series of layered sequences of nested U-shaped SiC_f/SiC shells, with a solid breeder/Be-pebble mixture between each shell. Every shell is fitted to the rear zone which includes Be and SiC reflectors and a SiC plenum. Helium coolant channels are embedded in the composite U-shells.

The DREAM (Drastically Easy Maintenance) concept, developed by JAERI in Japan, is divided into 16 sectors based on modular "mushroom-shaped" components assembled to form the blanket. In each module, two "mushroom" top (near-plasma) capsules constitute the breeding volumes (Be and LiO_2). The helium coolant stream, coming from the inlet circuit directly into the first wall box and then flowing through the inner capsules has the function of tritium recovery.

The TAURO design, developed by the CEA, has focused on the outboard blanket segment, which is divided into three straight 3.5 m-high modules along the poloidal (polar) direction and attached on a common, thick back-plate but cooled independently. Each module is composed of five subunits along the toroidal direction, containing the Pb–17Li that will have the multiple functions of cooling media, neutron multiplier, tritium breeder and carrier.

These studies were based on the materials database on industrial SiC/SiC composites. These works and additional activities covering other material science topics permitted a ranking of R&D priorities necessary to improve the characteristics of current SiC/SiC composites. First priority is obviously the identification of a radiation resistant composite, that is able to keep its physical (e.g., thermal conductivity) and mechanical properties above certain values under intense neutron irradiation at high-temperatures (873–1273 K). A properties database should be completed, covering the entire operating temperature range, in order to supply designers with comprehensive data. Component related issues are compatibility with coolant media, hermeticity, low activation joints stable under neutron irradiation and mock-up construction studies. In the following sections, some of these issues are discussed in more detail.

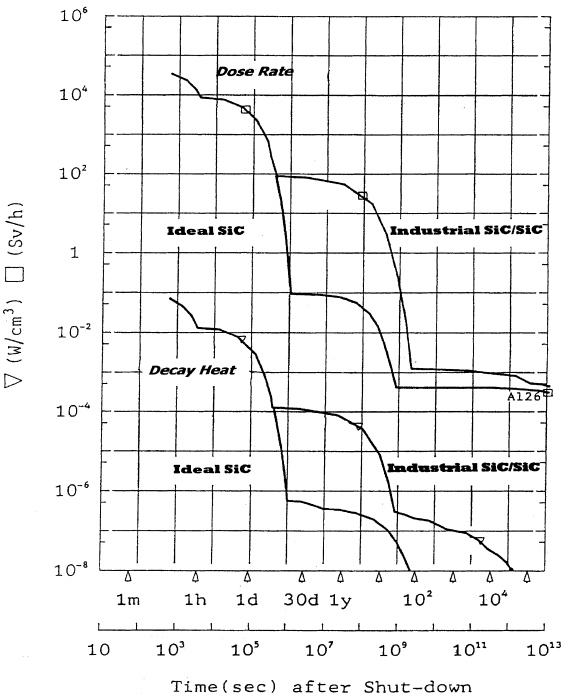

Fig. 1. Induced radioactivity in SiC after exposure in a fusion power reactor first wall (4.15 MW/m^2 for 2.5 y) [9].

3. Low activation

The low induced activation is one of the main merits of silicon carbide when its application in fusion technology is considered. The use of low activation materials (LAMs) is seen as a requirement determinant to satisfy the demand of an inherently safe and environmentally beneficial energy system. Fig. 1 illustrates the calculated induced radioactivity of silicon carbide after an exposure in a typical fusion reactor spectrum [9]. For idealised SiC it is evident that the short-term reduction of radiological parameters, the dominant contribution of long half-life ^{26}Al (half-life: 7.2×10^5 years) in the longer term and, when industrial SiC-based composites are considered, the detrimental effect of impurities are important.

In the long-term, production of ^{26}Al dominates the activation via the reactions

$$\begin{aligned} &\text{(a)}\ \ {}^{28}\mathrm{Si}(\mathrm{n},\mathrm{d})\ {}^{9.35\ \mathrm{MeV}}\!\!\rightarrow\ {}^{27}\mathrm{Al}(\mathrm{n},2\mathrm{n})^{13.1\ \mathrm{MeV}}\!\!\rightarrow\ {}^{26}\mathrm{Al} \\ &\text{(b)}\ \ {}^{28}\mathrm{Si}(\mathrm{n},\mathrm{n}'\mathrm{p})\ {}^{11.6\ \mathrm{MeV}}\!\!\rightarrow\ {}^{27}\mathrm{Al}(\mathrm{n},2\mathrm{n})^{13.1\ \mathrm{MeV}}\!\!\rightarrow\ {}^{26}\mathrm{Al} \end{aligned} \quad (1)$$

The fact that these reaction chains are ignited by ^{28}Si, which is the most abundant isotope of silicon (93.3%) makes isotopic tailoring unrealistic. However, from the large values of the threshold energies (above arrows in Eq. (1)) it is concluded that large activation on a SiC structure will be significant only for the initial layer of the first wall, as neutron energies will be significantly moderated at the inner volume (Table 2) [2,9,10]. Recent calculations using updated libraries such as FENDL/A-2.0 note a reduction of almost a factor 10 in the production of the radionuclide Al-26 via (b) reaction [11]. Cross-sections used for the reaction were derived from improved theoretical approaches, however experimental validation still lacks. Confirmation of the former calculations will establish SiC-based CMCs as integral low activation materials.

As outlined, the radiological response of SiC_f/SiC will be strongly dependent on its impurity content, linked to processing routes of fibres and composite. At present, extensive assessment of impurity content for SiC-based composites has been carried out only for SiC (CVI) matrix composites [12–15]. Chemical analysis, charged particle analysis (CPAA) and neutron activation analysis (NAA) were used to quantify impurity content down to atomic parts per million (appm). In Table 3 a list of impurities is presented, as measured in different laboratories. From these results, it is ascertained that the processing of fibres and the CVI production route, though not specifically developed for fusion, already ensure a low impurity content.

The former data have been used as input for activation calculations [10,13,15–18], whose results are used to qualify the radiological response of current industrial materials. Tough different criteria have been proposed for low activation, some common points have been highlighted in the different evaluations found in literature [9–13,15–18]: (i) maintenance requires a radiation environment allowing operation of remote handled instrumentation; (ii) safety and public acceptance require minimal risks for in-plant workers and minimal hazards in case of accidents; (iii) the volume of radioactive waste should not exceed certain limits; (iv) recycling after 50 years is also mentioned, though for SiC this is not seen as economically reasonable, as raw materials are largely available. A comparison with other candidate low activation materials (LAMs) – e.g., low activation steels, vanadium alloys, titanium intermetallics – shows that after short (1 day) and medium periods (up to 50 years), SiC is clearly the best solution. In the long term (100 years), depending on the criteria, SiC CMCs are classified as Low Level Waste, or Intermediate Level Waste [10,15,17]. In addition, modified cross-sections for Al-26 production have not been considered, and will imply significant reduction of the residual activity long-term values of SiC-based materials.

Table 2
Low activation properties of Nicalon CG/SiC (CVI) composites [10]

	Limit [8]	SiC/SiC first wall	SiC/SiC blanket
Early dose (mSv/1 kg)–(mSv/10 kg)	<50	0.020–0.20	0.007–0.07
Dose rate inside the plasma chamber after 1 d (Gy/h)	10^4	2.4×10^2	4.4×10^1
Contact dose rate after 50 y (mSv/h)	LLW < 2 MLW < 20	1.5	0.62
Decay heat after 50 y (W/m^3)	LLW < 1 MLW < 10	<0.1	<0.1
Contact dose rate after 100 y (mSv/h)	RHR < 1 0 HOR < 0.01	0.45	0.19
Porposed waste management strategy		LLW	LLW

Early dose: 50 y committed EDE due to the first week of exposure.
Reference release: 1–10 kg of activated material.
Irradiation conditions: SEAFP2 outboard first wall and mean outboard blanket fluxes: 2 MW/m^2 for 5 y.

Table 3
Elementary composition of Nicalon™/SiC (CVI) composites: Neutron Activation Analysis (NAA)

Elementary composition (wt%)				
Element	NicCG/SiC(IAM-EU)-*Cerasep® N2-1* [12]	NicCG/SiC (ENEA-Italy)-*Cerasep® N2-1* [13,14]	NicCG/SiC (Japan)-*Cerasep® N2-1* [14]	Hi-Nic/SiC (Japan) [14,15]
Si	65.7 [b]	65.75	–	69.7 [b]
C	30.1 [b]	30.1	–	29.7 [b]
O	3.98 [b]	4.043	5.79	0.38
Ag	$<5.5 \times 10^{-6}$ [a]	1×10^{-5}	$<1 \times 10^{-6}$	$<9.5 \times 10^{-7}$
Al	2.5×10^{-3} [b]	6.25×10^{-4}	$<5.6 \times 10^{-5}$	5.6×10^{-5}
As	–	$<1.4 \times 10^{-6}$	1×10^{-5}	8.3×10^{-6}
Au	5.6×10^{-2}	6×10^{-6}	$<1.5 \times 10^{-7}$	3×10^{-7}
Br	–	–	$<4.7 \times 10^{-6}$	$<7 \times 10^{-6}$
Ce	1.5×10^{-5}	–	1.1×10^{-5}	5.3×10^{-5}
Cl	3.08×10^{-2}	3×10^{-2}	2×10^{-2}	2×10^{-2}
Co	$<3.6 \times 10^{-6}$ [a] 8.8×10^{-6}	4.4×10^{-5}	1.2×10^{-5}	2.9×10^{-6}
Cr	3.7×10^{-7}	3×10^{-7}	8×10^{-4}	2.1×10^{-4}
Cu	3.3×10^{-4} [a]	3.3×10^{-3}	$<1.5 \times 10^{-4}$	2.1×10^{-4}
Eu	2×10^{-4} [b] $<4.0 \times 10^{-7}$	–	6.6×10^{-8}	1.5×10^{-7}
Fe	1.2×10^{-3} [a] 2.3×10^{-3}	7.74×10^{-3}	4.0×10^{-4}	4.5×10^{-4}
Ga	–	–	4.8×10^{-6}	2×10^{-7}
Hf	$<1.1 \times 10^{-6}$	1×10^{-6}	1.2×10^{-6}	1.6×10^{-5}
Hg	–	–	$<6 \times 10^{-7}$	$<6 \times 10^{-7}$
K	8×10^{-4} [b]	8×10^{-4}	5.2×10^{-5}	8.2×10^{-5}
La	1×10^{-6}	1×10^{-6}	2.2×10^{-6}	2.1×10^{-6}
Mo	1.8×10^{-5} [a] 2.0×10^{-5}	4×10^{-4}	$<1.8 \times 10^{-4}$	2.2×10^{-5}
Mn	–	2.88×10^{-5}	$<2.2 \times 10^{-6}$	8×10^{-5}
N	6.2×10^{-2} [b]	6.2×10^{-2}	1.14×10^{-1}	1.0×10^{-2}
Na	1.15×10^{-3}	3.16×10^{-4}	3.2×10^{-5}	1.7×10^{-4}
Nb	$<5.0 \times 10^{-4}$ [b]	5×10^{-4}	–	–
Nd	$<1.0 \times 10^{-3}$ [b]	1.0×10^{-4}	$<9 \times 10^{-6}$	9×10^{-6}
Ni	5.5×10^{-4} [a]	2.36×10^{-4}	4.2×10^{-4}	8×10^{-5}
Os	$<3.0 \times 10^{-3}$ [b]	3.0×10^{-3}	–	–
Pb	4.1×10^{-5} [a]	4.13×10^{-5}	$<1.0 \times 10^{-4}$	2×10^{-4}
Sb	5.3×10^{-6}	5.3×10^{-6}	3.3×10^{-6}	1.5×10^{-6}
Sc	$<1.1 \times 10^{-7}$	–	7.6×10^{-7}	2.1×10^{-7}
Sn	$<6.4 \times 10^{-5}$ [b]	3×10^{-4}	–	–
Ta	$<1 \times 10^{-6}$	1×10^{-6}	$<1.1 \times 10^{-5}$	4.7×10^{-7}
Tb	$<2 \times 10^{-3}$ [a]	2×10^{-7}	–	–
Ti	6.0×10^{-5} [a] 8.0×10^{-4} [a]	1.06×10^{-4}	$<1.9 \times 10^{-4}$	1.9×10^{-4}
V	–	–	$<3 \times 10^{-5}$	$<3 \times 10^{-5}$
W	4.88×10^{-5}	4.88×10^{-5}	1.0×10^{-5}	1.0×10^{-5}
Zn	3.8×10^{-4} [b]	8.2×10^{-5}	1.8×10^{-5}	3.7×10^{-5}
Zr	2.3×10^{-5}	2×10^{-5}	1×10^{-4}	1×10^{-4}

Additional methods:
[a] CPAA – Charged Particle Activation Analysis.
[b] CHEM – Chemical Analysis.

4. Irradiation behaviour

4.1. Neutron irradiation

The main features of the mechanical behaviour for Nicalon™ fibre CG/SiC (CVI) composites following neutron irradiation that were first reported by Snead et al. [19], and also investigated at Institute for Advanced Materials/Joint Research Centre, Ispra, are illustrated in Fig. 2 [20]. At low fluences (1 dpa) a reduction of bending strength occurs, but a toughness increase is present. For 2–3 dpa accumulated damage doses

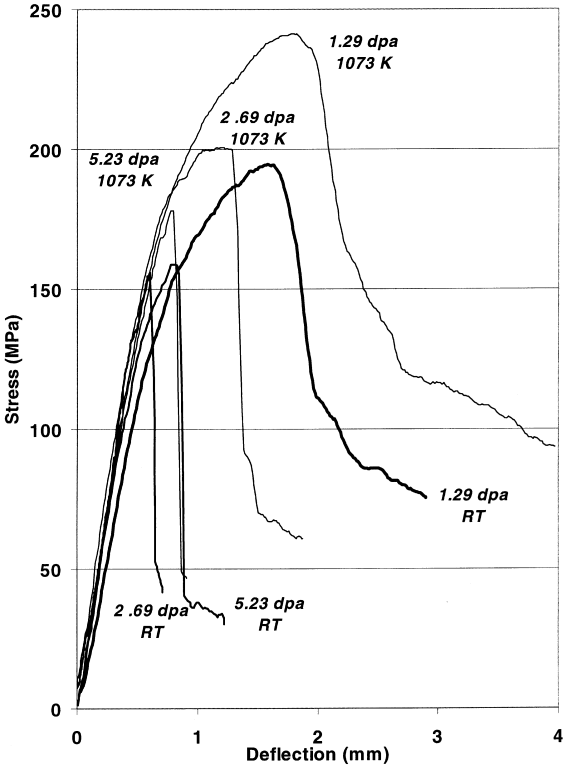

Fig. 2. Stress–displacement curves, at RT and 1073 K, for neutron irradiated Nicalon™ $_f$/SiC composites [20].

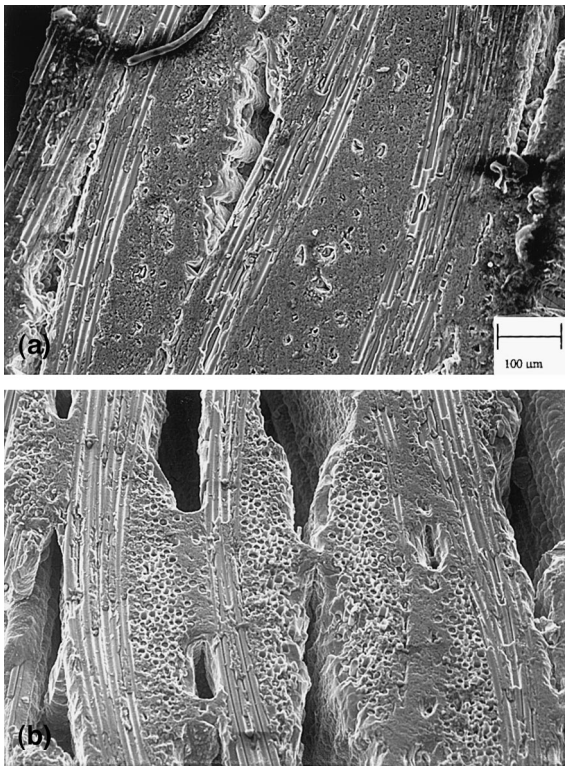

Fig. 3. Lateral surfaces of Nicalon CG™ $_f$/SiC (CVI) composite: (a) unirradiated and (b) neutron irradiated (1 dpa).

strength still decreases and, while matrix cracking still occurs prior to the maximum stress, the earlier toughening mechanisms are reduced. Also from Fig. 2, a recovery of the mechanical properties is observed at 1073 K. At these temperatures, partial recombination of point defects explains the observed improvement. Degradation of the mechanical properties of Nicalon™ fibre CG/SiC composites continues up to doses of 5 dpa, after which only minimal losses occur, as seen in the results for irradiated materials with accumulated damage doses up to 80 dpa [21,22].

The elementary mechanisms for the observed mechanical property behaviour can be derived from the features of the main composite phases. The matrix is a fully dense SiC with grain dimensions of 50 nm for isothermal CVI. For temperatures up to 1073 K, a decrease in swelling of the matrix with increasing temperature occur [21], in agreement with the earlier work of Price [23]. Conversely, the Nicalon fibre density increases and, for moderate fluences, becomes unable to withstand high loads following matrix crack initiation [24]. Such dimensional mismatch is shown in Fig. 3(a) and (b), where both differential dimensional responses of matrix and fibres are visible following neutron irradiation.

Two main mechanisms have been identified to account for the fibre degradation. For accumulated damage doses up to 1 dpa, fibre shrinkage is related to an irradiation-induced rearrangement of the glassy oxycarbide phase in the fibre, as observed for irradiated silica [24]. As a consequence of this rearrangement, the fibres pull away from the matrix making it impossible for the fibre/matrix interface to transfer load and take advantage of fibre strength in the composite. For fluences up to 43 dpa, mass losses, enhanced for carbon coated fibres, must be considered to fully account for the density increase [25]. These mass losses are to be related to the fibre microstructure, which consists of SiC crystallites (2–5 nm) and free carbon combined in an amorphous silicon oxycarbide phase. This composition does not correspond to a thermodynamic equilibrium state [26], which explains microstructural composite evolution during annealing treatments. For temperatures higher than 1473 K, chemical processes leading to an equilibrium state are thermally overpowered, details depending upon the surrounding atmosphere [27,28]. It seems that for irradiation below temperatures where thermal evolution begins, some chemical processes are, in some way, initiated by the energy incident particles.

4.2. Helium transmutation gas

In a fusion neutron spectrum, helium will be produced at the rate of about 1500 appm/MW a/m^2 in SiC, and its consequences on the properties of SiC/SiC composites should be considered. Scholz et al. [29] used a 39 MeV α-beam at the Ispra-Cyclotron to uniformly implant 2500 appm of He at 1173 K in a finite volume of flexure specimens. With the irradiated volume located along the tensile beam of the sample and submitted to the maximum load, a 38% decrease in the value of the three-point bending strength was reported as well as reduction in the displacement at maximum load [20]. Hasegawa et al. [30], using a similar experimental approach, also observed a decrease in the four point bending strength value of about 20% for specimens implanted with 150–170 appm He at 873 K.

Present understanding of microstructure effects of helium in SiC is limited. For SiC/SiC composites implanted with 2500 appm helium at 1173 K, an induced linear expansion of around 0.4% for the SiC (CVI) matrix was measured [31]. This is significantly higher than that expected if pure displacement damage is considered [21]. Isotropic swelling will lead the matrix to pull away radially from the fibres, hence accounting for the mechanical features referred to above. TEM analysis revealed no large helium agglomerations in the matrix, but along the carbon interface/matrix region small bubbles were visible [31]. Hi-Nicalon™ fibre/SiC composites uniformly implanted with up to 10 000 appm helium, at room-temperature, and annealed at 1673 K, contained helium bubbles only at the outer growth boundaries of the SiC (CVI) matrix [32]. These observations coupled with the swelling reported in [31] suggests that significant amounts of the uniformly implanted helium are remaining in the matrix at lower temperatures, and diffuse to the matrix boundaries to form large agglomerates for $T > 1673$ K. These observations are contrary to the earlier work of Sasaki [33], who claimed that there was higher helium mobility in sintered SiC, at temperatures as low as 1073 K, that explained He release from neutron irradiated SiC containing 0.1 wt% B. Allen [34] has studied the behaviour of helium in SiC, suggesting an enhanced stabilisation of point defects, which could account for the observed swelling at higher temperatures. Additional investigations, including refined microstructure analysis, are necessary to ascertain these mechanisms.

4.3. Irradiation creep

The creep behaviour of CMCs was summarised by Jones et al. [3], and results on thermal creep of SiC-based fibres was reported by Youngblood [35], concluding that the most favourable response is for enhanced crystalline fibres. On the other hand, irradiation creep of SiC CMCs data is limited. Only recently, Scholz investigated deuteron irradiation creep in torsion for CVD SCS-6 fibres, thus allowing an extrapolation of the results to the behaviour of the β-SiC (CVI) matrix of SiC CMCs [36,37]. A significant enhancement in creep deformation was observed in comparison with thermal creep. Creep rate linearly depends on the applied stress and dose rate and decreases with increasing temperature. The temperature dependence was related to the swelling of SiC, which is also diminishing at higher temperatures ($T < 1273$ K). A possible explanation proposed by Scholz for the observed creep is that a grain boundary sliding mechanism accommodated by stress induced preferential nucleation (SIPN) of dislocation loops [38]. At lower temperatures, a larger number of defects are present – in particular, mobile carbon interstials that can form small clusters [39]. At higher temperatures, interstial-vacancy recombination is thermally enhanced, thus limiting such cluster nucleation. In this way, grain boundary sliding is also blocked by the absence of accommodation arising from the SIPN process.

4.4. Thermal properties

Enhanced thermal conductivity will be mandatory for the use of SiC based CMCs as a fusion structural material. The value of the thermal conductivity should comply with design requirements for heat removal and minimisation of thermal stresses. Thermal properties of silicon carbide are highly dependent on the microstructure. At room-temperature, thermal conductivity of SiC can vary from 1 W/mK for nano crystalline fibres up to 490 W/mK for high-purity single crystal SiC, according to impurity content, lattice defect density, average grain size, porosity and the presence of amorphous and/or interfacial phases.

For current industrial Nicalon CG™ fibre /SiC (CVI) composites, the thermal properties are relatively modest, e.g., 12 W/mK for current 3-D Nicalon CG™ fibre /SiC (CVI). This is due to the low thermal conductivity of Nicalon CG fibre [40], matrix porosity, micro-cracks and grain size. In Fig. 4 the dependence of thermal conductivity on the porosity for 2-D Nicalon CG™ fibre/SiC (CVI) composites is shown. Moreover, a theoretical thermal conductivity for SiC (CVI) has a value of 40.1 W/mK, calculated using fibre conductivity and an extrapolated value for a non-porous matrix, is significantly lower than, e.g., 300 W/mK reported for SiC CVD [41]. Reduced grain size (∼50 nm) [42], lattice defects and growth interlayers due to the matrix infiltration process are likely to account for this difference. Simple calculations of the thermal stress factor, used to qualify the ability of a material to comply with induced thermal loads, predict a value of around 0.04 MPa/Wm for unirradiated Nicalon CG™ fibre/SiC (CVI) which is encouraging when compared with other candidate LAMs

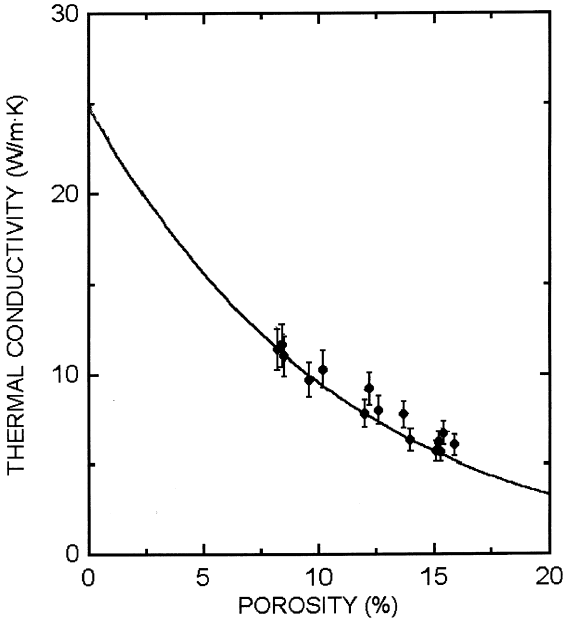

Fig. 4. Thermal conductivity vs. porosity for 2-D Nicalon CG™ $_f$/SiC (CVI) composites. The line represents a fitting for the experimental points, using a 'self-consistent model' which includes contributions of the porosity shape and orientation.

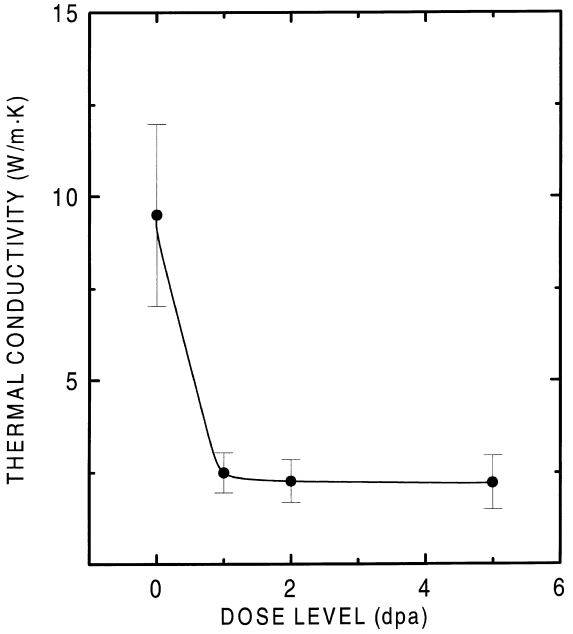

Fig. 5. Thermal conductivity of neutron irradiated 2-D Nicalon CG™ $_f$/SiC vs. dose level.

(low activation steels, vanadium alloys). However, if a SiC/SiC structure will contain a cooling media then improved thermal conductivity will be necessary.

Neutron irradiation will significantly reduce thermal conductivity. Room-temperature thermal conductivity for 2-D Nicalon CG™ fibre/SiC (CVI) irradiated at 1023 K shows a sharp reduction to 20% of the initial values for only 1 dpa damage level, but without significant degradation for higher doses (Fig. 5) upto 24 dpa [21]. Hollenberg et al. [21] observed that a partial recovery occurred for the thermal conductivity for irradiated materials after thermal annealing, depending on irradiation temperature, with the best result being registered at 1073 K. Youngblood et al. [43], from studies carried out on monolithic SiC CVD, reported a significant decrease for samples irradiated up to 43 dpa at 1273 K, demonstrating that thermal annealing only permitted an improvement of up to 50% of the initial values. This seems to suggest that neutron induced damage at 1273 K, for such high doses, also comprise other types of damage than point defects or small clusters, which are normally recovered during thermal annealing. Further studies, for lower irradiation temperatures, are necessary to confirm these effects.

5. Technological issues

5.1. Advanced fibres and interfaces

As described above, the key to the radiation performance of state-of-the-art SiC/SiC composites lies in the stability of the fibres. Some of the fibres under consideration to be used as reinforcement in SiC CMCs are listed in Table 4. The most widely studied and developed are the commercial SiC-based Nicalon™ fibres, derived from a polymer precursor process [44]. This fibre is

Table 4
Advanced SiC fibres – Main characteristics [2,49]

Property	Nicalon CG	Hi-Nicalon	Nicalon S	Sylramic
Av. Diameter (μm)	14	12–13	11	10
Density (g/cm^3)	2.55	2.74	3.0	3.1
Grain size (nm)	1–2	5–10	11	500
Oxygen content (wt%)	11–14	0.5	0.2	Not reported
C/Si ratio	1.31	1.39	1.05	1.0
Young's Modulus (GPa)	190–220	270	420	400–420

melt-spun from a silicon and carbon containing polymer and cured in oxygen to produce the SiC fibre. This reaction produces substantial residual oxygen and carbon, leading to the earlier described Nicalon CG microstructure, that is responsible for its lack of thermal and irradiation stability. This motivated the interest in the newer lower oxygen "Hi-Nicalon™" fibre. However, even for the <0.5% oxygen Hi-Nicalon™, a radiation induced densification of the fibre [45] occurs leading to a degradation in composite performance under irradiation [46]. While this degradation is similar to the degradation seen in the ceramic grade composites previously studied, the Hi-Nicalon fibre showed slightly less loss in strength and higher unirradiated and irradiated strength values as compared with the ceramic grade material. These observations may be explained qualitatively by the lower absolute densification of the Hi-Nicalon™ as compared with the ceramic grade material and the larger dose required for noticeable densification to occur [45].

The next improvement in radiation performance for SiC composites may come from the next generation of Nicalon™ fibres. A stoichiometric Nicalon™ designated "Type-S" is now available in research quantities. This fiber is near full density and contains essentially no oxygen and should therefore swell essentially like the CVD SiC matrix of the composites being studied. The type-S fibre has C/Si ratio of nearly one, where as the Hi-Nicalon™ has C/Si of 1.4. To date there is not sufficient information to comment on the mechanical properties of such a composite, though work is underway in the fusion program internationally to produce and irradiate such material.

While the culprit for the degradation of SiC composite performance has been the densification of the SiC-based fibres currently in use, the actual weak link is the interface. Irradiation behaviour highlighted the sensitivity of the composite to the changes on the fibre/matrix interfacial region, though these are in first place dictated by fibre shrinkage. It is well known [47] that the commonly used carbon interphase material will undergo large anisotropic swelling which is anticipated to be detrimental to irradiated composite performance. An additional concern is related to the insufficient corrosion resistance, in the long-term, as reported by Jones et al. [48]. Alternative interface approaches specifically developed for irradiation testing, are pseudo-porous SiC and multiple layers of SiC (e.g., multilayer SiC). Composites with these interfacial layers have shown unirradiated and irradiated performance comparable to the carbon interphase materials. [45].

5.2. Matrix processing methods

Alternative matrix processing routes are available, although studies focussing on structural fusion applications have been limited for these types of materials. Polymer infiltration and pyrolisis (PIP) for matrix synthesis uses an organo-metallic polymer to form a refractory matrix in CMCs. The main steps of the PIP fabrication process include infiltration and consolidation of the fibrous preform with a polymer precursor; curing to prevent melting during subsequent processing; pyrolisis and ceramic conversion. A high ceramic-yield precursor is desirable to limit extensive pore growth and volume reduction during the polymer-ceramic conversion step. PIP processing is less expensive than CVI and can be carried out at relatively low-temperatures. In addition, complex shapes can be prepared using standard polymer infiltration processing techniques. Unfortunately, current PIP matrices exhibit low thermal properties and stiffness when compared with composites produced by CVI. Moreover, residual oxygen content and poor crystallinity in PIP derived material represent significant drawbacks under irradiation, as observed for Nicalon CG fibres. Donato et al. [50] have used SiC nanopowders with a polymer precursor to form a SiC matrix. This composite exhibited good mechanical properties: in particular, high strain-to-failure and toughness. Availability of advanced fibres, able to cope with higher pyrolisis temperatures, will permit to reduction of oxygen content and allow increase in crystallinity and stiffness for these CMCs. An improved hybrid method, combining PIP and CVI, permitted fabrication of a SiC/SiC composite with good crystallinity and a room-temperature thermal conductivity as high as 45 W/mK [51]. Annealing temperatures of 2073 K and use of Be and B additives were necessary to improve crystal growth and thermal properties. The fibrous reinforcement must be stable at these high annealing temperatures. This was achieved through the use of SiC fibres obtained by chemical vapour reduction (CVR) of graphite (Celion™) fibre precursor.

Reaction sintered Hi-Nicalon™ fibre/SiC composites have been developed in Japan, where also small components were produced [52]. The resulting SiC matrix contained some free silicon (15–20% of matrix volume), and the fibre/matrix interface has boron nitride (BN). The resulting composite exhibited extremely low porosity and high room-temperature thermal conductivity (40 W/mK). Manufacture via reaction sintering is relatively simple as the several cycles of infiltration associated with CVI and PIP are substituted by a single step of slurry impregnation, slip casting and reaction sintering at 1723 K in vacuum for 5 h. For fusion applications, consequences of the presence of excess silicon in the matrix must be evaluated: in particular, its response to irradiation.

5.3. Joining

SiC/SiC structures in an FPR, as summarised earlier in the description of the design projects, will be fabri-

cated from small, basic components. In the case of the ARIES and DREAM studies, a high degree of modularity is proposed. In the case of TAURO, fabrication will imply that each submodule will be assembled from small, simply shaped parts. Thus, the availability of reliable joints is critical, when considering the technological feasibility of SiC/SiC structures.

General requirements can be drawn for acceptable joints. Such compounds must be built up with low activation elements, should have refractory characteristics to operate at temperatures up to 1273 K, stability under irradiation and be chemically compatible, at high-temperatures, with the coolants adopted. More specific requirements for the joints are linked to the specific design adopted. TAURO and ARIES will require load-bearing capabilities during irradiation, whilst for the DREAM project it is envisaged that the joint additionally function as a permeation barrier.

In Table 5, joints under consideration for fusion structural applications are summarised. Some of the joints were performed on monolithic SiC, as a preliminary step for their application in composites. Jones et al. [53] utilised an in situ displacement reaction for joining polished α-SiC. This process begins with TiC and Si powder but results in a joint comprised of Ti_3SiC_2 + -SiC after reaction at 1473–1673 K with a joint shear strength of 50 MPa. In the works of Donato et al. [54,55], a SiOC glass was used to join α-SiC and a 2-D SiC/SiC (CVI) resulting in shear strength values of 37 MPa and 3–15 MPa, respectively. This illustrates that the transition from monolithic to composites is not straightforward, since composite morphology, in particular open porosity raises additional issues for the joint consolidation.

A brazing method for joining 3-D SiC/SiC has been developed at CEA [56]. This brazing compound (BraSiC®) made of low activation elements was designed to work at elevated temperatures and to be compatible with SiC. Brazing was completed at 1673 K with reported room-temperature joint strengths as high as 200 MPa.

Ferraris et al. [57] produced brazed joints of SiC/SiC using zinc borate glass at 1473 K. A room-temperature shear strength of 15 MPa was obtained. Using silicon metal, different joint thicknesses are possible, with room-temperature shear strength of 22 MPa. Encouraging results were also obtained using glass-ceramics to bond SiC CMCs, with a value reported 33 MPa for room-temperature shear strength [58].

Future studies should include high-temperature testing and assessment of the irradiation features for these compounds, as well as their influence on the mechanical response when incorporated in CMCs mock-up components.

6. Strategy and future work

The development of radiation resistant CMCs emerges as the main objective for future studies. Present-day knowledge suggests that enhanced irradiation resistance will depend on the availability of quasi-stochiometric SiC and avoiding the presence of glassy/amorphous phases. The progressive availability of advanced fibres, with high thermo-chemical stability will require deep engagement of the industry in the technological development of CMCs, and will require optimisation of current matrix/composite production routes.

Table 5
Joints under consideration for SiC CMCs

Methods	Joined materials	Joint	Processing	Joint thickness (nm)	τ_{RT} (Mpa)	Comments and issues
Pre-ceramic polymer use	α-SiC	SiOC glass	200 + 1473 K Precursor: methyl hydroxyl-siloxane (SR 350)	0.002–0.004	37	Shrinkage due to ceramic conversion
	2-D SiC/SiC			0.002–0.004	3–15	Composite morphology porosity
Brazing	3-D SiC/SiC	BraSiC® H	5 min 1613 K	0.4	70	Porosity
			(High vaccum)	0.1	370	Seal-coat of the composites
		BraSiC® V		0.1	190/200	
	2-D SiC/SiC	Si sheet	90 min 1693 K	1	22	
	2-D SiC/SiC	Glass Ceramics	–		13/33	
Displacement reactions	Hexalloy SiC	SiC + Ti_3SiC_2	De-bindering at 673 K (Argon) Anneal 1473–1673 K, 20 Mpa (Argon)	0.1	50	Composite joints

Enhanced crystal grain size would be desirable, though the resulting thermal behaviour and sensitivity to transmutation gases (e.g., He) should be further investigated.

In parallel with materials development, a substantial effort must be carried out to address technological issues such as:

(a) Refinement of current design studies perhaps developing a future common SiC CMCs FPR concept;

(b) Feasibility studies including mock-up manufacture, mechanical testing, joint development, compatibility and hermetic properties;

(c) Extension of the material database in order to provide designers with reliable data on mechanical and physical properties.

The substantial effort implicit in the former statements requires an increased collaboration of different laboratories, in particular for irradiation campaigns, access to TEM/HREM centres and definition of extended design requirements.

References

[1] P. Fenici, H.W. Scholz, J. Nucl. Mater. 212–215 (1994) 60.
[2] L.L. Snead, R.H. Jones, A. Kohyama, P. Fenici, J. Nucl. Mater. 233–237 (1996) 26.
[3] R.H. Jones, D. Steiner, H.L. Heinisch, G.A. Newsome, H.M. Kerch, J. Nucl. Mater. 245 (1997) 87.
[4] A.G. Evans, F.W. Zok, J. Mater. Sci. 29 (1994) 3857.
[5] S. Sharafat, F. Najmabadi, C.P.C. Wong, the ARIES team, Fusion Eng. Design 18 (1991) 21.
[6] S. Pérez Ramirez, A. Caso, L. Giancarli, N. Le Bars, G. Chaumat, J.F. Salavy, J. Szczepanski, J. Nucl. Mater. 233–237 (1996) 1257.
[7] S. Ueda, S. Nishio, Y. Seki, R. Kurihara, J. Adachi, S. Yamazaki and the DREAM design TEAM, these Proceedings.
[8] L. Giancarli, CEA Internal Report, DMT 97/400, 1997.
[9] P. Rocco, M. Zucchetti, EuroReport EUR 14805 EN, 1992.
[10] E.V. Dyomina, P. Fenici, V.P. Kolotov, M. Zucchetti, these Proceedings.
[11] E.T. Cheng, in: Proceedings of the ICFRM8, 1997.
[12] H.W. Scholz, M. Zucchetti, K. Casteleyn, C. Adelhelm, J. Nucl. Mater. 212–215 (1994) 665.
[13] A. Donato, M. Pillon, R.A. Forrest, in: P. Fenici, A.J. Frias Rebelo (Eds.), Proceedings of the First IEA International Workshop on SiC/SiC Ceramic Composites for Fusion Structural Applications, EUR 1375 EN, 1997, p. 43.
[14] A. Caso, LAM6 Meeting Minutes, Lisbon, 1997.
[15] Y. Seki, T. Tabara, I. Aoki, S. Ueda, S. Nishio, R. Kurihara, these Proceedings.
[16] N. Taylor, C. Forty, W. Han, I. Cook, C. Clair, in: C. Varandas, F. Serra (Eds.), Fusion Technology 1996 – Proceedings of 19th SOFT, North-Holland, Amsterdam, 1997, p. 1831.
[17] C.B. Forty, I. Cook, UKAEA Report FUS 365, 1997.
[18] P. Rocco, M. Zucchetti, Fusion Eng. Design 15 (1992) 235.
[19] L.L. Snead, S.J. Zinkle, D. Steiner, J. Nucl. Mater. 191–194 (1992) 566.
[20] A.J. Frias Rebelo, H.W. Scholz, H. Kolbe, G.P. Tartaglia, P. Fenici, these Proceedings.
[21] G.W. Hollenberg, C.H. Henager, Jr., G.E. Youngblood, D.J. Trimble, S.A. Simonson, G.A. Newsome, E. Lewis, J. Nucl. Mater. 219 (1995) 70.
[22] R.H. Jones, C.A. Lewinsohn, G.E. Youngblood, in: IEA/Jupiter Joint International Workshop on SiC/SiC Ceramic Composites for Fusion Structural Applications, 1997, Sendai, Japan.
[23] R.J. Price, J. Nucl. Mater. 33 (1969) 17.
[24] L.L. Snead, M. Osborne, K.L. More, J. Mater. Res. 103 (1995) 736.
[25] G.E. Youngblood, R.H. Jones, A. Kohyama, L.L. Snead, these Proceedings.
[26] N. Mozdzierz, M. Backhaus-Ricoult, Revue des Composites et Matériaux Avancés, 3, hors-serie, 1993, p. 49.
[27] M. Backhaus-Ricoult, N. Mozdzierz, J. Mater. Sci. 30 (1995) 3487.
[28] C. Labrugere, A. Guette, R. Naslain, J. Eur. Ceram. Soc. 17 (1997) 623.
[29] H.W. Scholz, P. Fenici, A.J. Frias Rebelo, in: P. Jung, H. Ullmaier (Eds.), Proceedings of IEA International Symposium on Miniaturized Specimens for Testing of Irradiated Materials, Julich, Germany, 1995, p. 201.
[30] A. Hasegawa, M. Saito, K. Abe, R.H. Jones, in: P. Fenici, A.J. Frias Rebelo (Eds.), Proceedings of the 1st IEA International Workshop on SiC/SiC Ceramic Composites for Fusion Structural Applications, EUR 1375 EN, 1997, p. 157.
[31] H.W. Scholz, A.J. Frias Rebelo, D.G. Rickerby, P. Krogul, W.E. Lee, J.H. Evans, P. Fenici, these Proceedings.
[32] A. Hasegawa, M. Saito, K. Abe, Y. Miwa, S. Hamada, these Proceedings.
[33] K. Sasaki, T. Yano, T. Murayama, T. Iseki, J. Nucl. Mater. 179–181 (1991) 407.
[34] W.R. Allen, J. Nucl. Mater. 210 (1994) 31.
[35] G.E. Youngblood, R.H. Jones, Fusion Reactor Materials Semiannual Progress Report for period ending 30 June, DOE/ER-0313/22, p. 81.
[36] R. Scholz, A.J. Frias Rebelo, F. Dos Santos Marques, in: P. Fenici, A.J. Frias Rebelo (Eds.), Proceedings of the 1st IEA International Workshop on SiC/SiC Ceramic Composites for Fusion Structural Applications, EUR 1375 EN, 1997, p. 151.
[37] R. Scholz, J. Nucl. Mater., accepted for publication.
[38] R. Scholz, these Proceedings.
[39] T. Yano, T. Iseki, Philos. Mag. 27 (1990) 67.
[40] J.J. Brennan, L.D. Bentsen, D.H. Hasselman, J. Mater. Sci. 17 (1982) 2377.
[41] Silicon Carbide CVD®, Properties and typical values, Morton Advanced Materials, Woburn, MA, USA.
[42] L. Fabbri, E. Scaffé, J. Nucl. Mater. 212–215 (1977) 835.
[43] G.E. Youngblood, J. Senor, Fusion Reactor Materials Semiannual Progress Report for period ending 30 June, DOE/ER-0313/22, p. 75.
[44] S. Yajima, J. Hiyashi, M. Omori, Chem. Lett. 9 (1995).
[45] L.L. Snead et al., J. Nucl. Mater., accepted for publication.

[46] L.L. Snead, M. Osborne, presented at 8th Int. Conf. on Fusion Reactor Materials, Sendai, Japan, 1997.
[47] B.T. Kelly, The Physics of Graphite, Applied Science Publishers, Barking, 1981.
[48] R.H. Jones, C.H. Henager Jr., P.F. Tortorelli, J. Organomet. 45 (12) (1993) 26.
[49] R.H. Jones, L.L. Snead, A. Kohyama, P. Fenici, in: Proceedings of ISFTN-4, Tokyo, Japan, in press.
[50] A. Donato et al., in: C. Varandas, F. Serra (Eds.), Fusion Technology 1996 – 19th SOFT, Lisbon, North-Holland, Amsterdam, 1997, p. 1379.
[51] J.C. Whiters, W. Kowbel, R. Loufty, G.E. Youngblood, C. Wong, in: P. Fenici, A.J. Frias Rebelo (Eds.), Proceedings of the First IEA International Workshop on SiC/SiC Ceramic Composites for Fusion Structural Applications, EUR 1375 EN, 1997, p. 69.
[52] A. Sayano, C. Sutoh, S. Suyama, Y. Itoh, S. Nakagawa, presented at 8th Int. Conf. on Fusion Reactor Materials, Sendai, Japan, 1997.
[53] R.H. Jones, G.E. Youngblood, C.H. Henager Jr., M.L. Hamilton, H.L. Heinisch, C.A. Lewinsohn, in: P. Fenici, A.J. Frias Rebelo (Eds.), Proceedings of the First IEA International Workshop on SiC/SiC Ceramic Composites for Fusion Structural Applications, EUR 1375 EN, 1997, p. 1.
[54] A. Donato, P. Colombo, M.O. Abdirashid, in: P. Fenici, A.J. Frias Rebelo (Eds.), Proceedings of the 1st IEA International Workshop on SiC/SiC Ceramic Composites for Fusion Structural Applications, EUR 1375 EN, 1997, p. 107.
[55] A. Donato et al., in: C. Varandas, F. Serra (Eds.), Fusion Technology 1996 – 19th SOFT, Lisbon, North-Holland, Amsterdam, 1997, p. 1375.
[56] L. Giancarli, J.P. Bonal, G.L. LeMarois, J.P. Salavy, in: P. Fenici, A.J. Frias Rebelo (Eds.), Proceedings of the 1st IEA International Workshop on SiC/SiC Ceramic Composites for Fusion Structural Applications, EUR 1375 EN, 1997, p. 35.
[57] M. Ferraris, M. Salvo, C. Isola, M.A. Montorsi, in: P. Fenici, A.J. Frias Rebelo (Eds.), Proceedings of the 1st IEA International Workshop on SiC/SiC Ceramic Composites for Fusion Structural Applications, EUR 1375 EN, 1997, p. 113.
[58] M. Ferraris, M. Salvo, C. Isola, M.A. Montorsi, A. Kohyama, these Proceedings.